Vibration Injury Network

Research Network on Detection and Prevention of Injuries due to Occupational Vibration Exposures

Development and Analysis of a Finite Element Model for the Group L5, S1 Disk using a Loading Model Simulating Whole-body Vibration

Appendix W3F to Final Report

May 2001

EC Biomed II concerted action BMH4-CT98-3251

Dr. P. Goudas[1], MD, Prof. M. H. Pope[2] Dr. V. Macropoulos[3], MD, Dr. G. Labeas[1]

and Prof. C. L. Goudas[1],

[1] Studium of Mechanics, University of Patras, Patras, Greece.

[2]Liberty – Worksafe Centre, Department of Environmental & Occupational Medicine, University of Aberdeen, Aberdeen, Scotland.

[3]Hellenic Institute for Occupational Health and Safety, Athens, Greece.

ABSTRACT

The group of spine elements L5, L5/S1 disc, and S1 is treated as an isolated body by application of the free-body principle, upon which external and inertial time-dependent or repetitive shock forces are applied. The material properties of the bodies considered are those given in literature. The method used for computing the impact of loading of this composite unit is that of creating a FE model. The model developed is made of 14902 3-D solid 8-node elements and will be extensively used for multidirectional loading. It is applied upon the upper surface of L5. Other loads, including non-axial ones are considered. By application of repetitive loading upon the group where the nth load is applied upon the geometry of the group as this is deformed by the (n-1)th load we study the impacts in cases of resonance and non-resonance between the natural frequency of the group and the frequency of the external vibration. The results of vertical loading by 0.4 Mpa, covering the 3-D displacements, the normal and shear stresses developed, and the equivalent stress (Von Mises) developed at all nodes of the vertebra L5 and the L5/S1 disk (in mm) are given.

Presented at the 1st International workshop "Modelling of Spinal Loads Associated with Vibration and Shock - State of the Art, Critical Assessment, Application, and Research Needs", Berlin, October 1999

1. Introduction.

The FE Analysis treatment of the intervertebral disks of the lumbar section presented in our previous paper (Goudas P et al[1]) for the particular case of L5/S1 disk, is extended in this paper for the group of the vertebrae L5 and S1 and the in-between disk. The same basic assumptions, objectives, methods and loading models are applied for this group of the human lumbar section. FE analyses of body parts known a priori to develop local deformations of maximum linear dimensions occasionally less than 1% of the maximum linear dimension of the part (e.g. disk hernia) enforce the use of highly detailed partitioning so as to enhance such deformations upon loading. Also, the assumption that simulation of loading corresponding to vibration conditions is achieved by applying to the FE model a second, third and so on, fixed loading at a state of the body with part of the deformation caused by the previous loading still present, is here applied.

All introductory comments in our previous paper[1] apply to this contribution and hence will not be repeated here. The results reported in that paper[1], where the intervertebral disk L5/S1 was isolated and analysed, are in fact reproduced in the present contribution where the same disk is no longer isolated but part of a larger group, and this serves as an indication of coherency of the analyses performed.

This paper reports on the FE model developed, the material properties adopted, the loading applied to the model and the strain results obtained and a model of loading simulating condition of WBV suitable for cases of resonance and non resonance of vibration frequency to the natural frequency of the human body.

2. The FE Model.

The detailed FE model developed for this work is based upon fine, small step CT scans of the lumbar section sited above. We used CT scans of the lumbar region of 20 healthy men 20-40 years old, 1,65-1,80 meters tall. The scans were collected from the Medical School of the University of Patras and the output was first digitised and then expressed into

Cartesian co-ordinates of a suitable number of section boundary points sufficient for detailed presentation of each and all three lumbar bodies under consideration. The model developed is made of 14902 3-D solid, 8-node elements.

The perspective view from top-front of the FE model developed for spinal group L5, L5/S1 disc and S1 is shown in Fig. 1. The whole group, considered isolated as a free body by replacement of the reaction forces applied upon it by adjacent parts including muscles, by using boundary conditions, is loaded at peak values of the inertial vibration forces and analyzed for the developed stresses and element displacements using the ANSYS commercial version.

The perspective view from top-front of the upper segment of the vertebra S1 is presented in Fig. 2. Since this vertebra will be considered in the analysis as clamped, only the segment shown in this Fig. is necessary for formulating the FE model of the group. The free-body principle is applied to disengage the segment treated from the rest body of S1.

In Fig. 3 we see the perspective view from top-front of the vertebra L5 as it is included in the FE model appearing in the total Figure 1. The linear dimensions of the elements for this vertebra, as well as for S1, are not as small as those used for the model of the corresponding intervertebral disc. The expected deformations of the vertebrae are small and uniform so as to be detectable from a cruder element partition.

In Fig. 4 we show the perspective view from top-front of the L5/S1 intervertebral disc. The viewpoint is the same as that used for presenting Figs. 1-3. This component of the group L5 vertebra, L5/S1 disk, S1 vertebra, is modeled with considerably finer elements on account of its elastoplastic properties which permit small-scale distortions and failures (raptures). The loading of this part is no longer external and hence it is treated as a free body.

3. Material Properties.

The material properties expressed by the measure of elasticity E for the cortical, the cancellous parts of the vertebral bones and for the fibrous and fluid parts of the intervertebral disk were taken to be

cortical bone: E= 12000Mpa,

cancellous bone: E= 100Mpa,

while the index n was given the value 0.3. The values of E for the fibrous and fluid parts are given in our previous paper[1]. Investigation of the impact of variations of E for some or all parts of the group under study, and mainly variations within the same body, such as the inhomogeneity assumed and studied[1], are simple to perform but not reported in this paper.

4. Boundary conditions.

The lower part of the S1 was clamped upon the pelvis so as the corresponding nodes to be immovable. The disc L5/S1 was taken to have its lower face fixed and in complete coincidence with the upper face of S1 while its lower face attached to L5.

The essential detail of the role of the down bent processes of L5 contacting at the corresponding parts S1 and establishing lines of two-way stress transfer between the two vertebrae, gap elements were used to model the contacts of L5 and sacral bone. These gap elements are included in the total model already presented.

The surrounding tissues (muscles, tendons, ligaments) were transformed in stability forces, damping factors and boundary conditions according to their anatomical properties and positions. The muscles were transformed in three different statuses, i.e. totally relaxed, half flexed and flexed in their maximum tension. The corresponding forces and elasticities were found in literature.

5. Loading.

The case treated in Phase 1 of the experiments run was that of uniform pressure of 0.4 and multiplicates of this pressure (0.8, 1.2, 1.6 etc) Mpa applied upon the upper face of L5. In Phase 2, the experiments run where based upon a loading model simulating vertical compression caused by vibration. Since performance of FE analysis with time-dependent loading is extremely difficult for the present computer capabilities and the large number of elements at hand, the loading model that simulates time-dependent forces was base upon discretization of the time parameter. Thus, we adopt a time step h, and repeat the FE analysis at time instances t=h, t=2h, etc. using each time the new value of the loading. Critical in this procedure is the size of h and the strain condition of the body model at the time instant (n-1)h at which the new load will be applied for the instant nh, particularly when h cannot be selected small or representing suitable time interval of repetitive occurrence of critical loading. The approach used in this paper is to approximate loading conditions of the same peak compression values and assume that the strain condition of the body at the instant of second, third, etc, application corresponds to the strain condition that resulted by the first load application multiplied by a coefficient k, with 1>k>0. Thus if $\mathbf{P}$ is the fixed pressure load used and $\mathbf{u}_{ijk}$ is the vector strain that resulted from the 1st application, then at the 2nd application the vector position $\mathbf{r}_{ijk}$ of the node N_{ijk} will be assumed to be at the position $\mathbf{r}_{ijk}+k\mathbf{u}_{ijk}$, where k=0.9, 0.8, 0.7, . . ., 0.1. Varying $\mathbf{P}$ at each new analysis generalises the simulation model, while relating its values to peak acceleration data such as these by Seidel et al[2] permits comparisons and testing of the model.

Since resonance between the natural frequency of the vibrating body and the frequency of the external time-dependent (vibration) load, as a rule, causes extreme damage, the question that rises is whether this simulation model can also simulate such phenomena. The answer is affirmative since application of n successive FE analyses for $\mathbf{P}$ = constant and k = 1 we have a case of perfect resonance. The farthest we can go away from resonance is when $\mathbf{P}$ = constant and k = 0 since at each analysis the body is found in its original condition.

Perfect resonance simulated by this loading model is obviously equivalent to shock loading since application of a load **P** n times in successive steps but under resonance assumption brings about the same result as a single load of size n**P** applied once. Hence, the load model presented here is suitable for covering also the case of shock loading. The impacts of resonant time-dependent and single shock loading are shown to be the same, as they are in reality.

In Phase 3 the experiments run where based upon a loading model simulating non-vertical compression, i.e. the loading applied on the upper surface of the L5 vertebra was the starting 0.4 Mpa pressure and multiplicates of the initial load in different angles (10 to 45 degrees) with the vertical (z) axis, on the z-x plane. This form of loading created a far more stressfull condition on all elements of the disk and showed a more important protective role of the damping and boundary conditions of the surrounding tissues. In Phase 4, loading was tested in different angles with (z) axis but on the z-y plane, giving similar results with Phase 3. In Phases 3 and 4 there were observed many plastic deformations of the disk in different areas, depending on the angles and loadings used. In Phase 5 the model was deformed before it was loaded as if it was a case of different stances of the spine, namely one bent forward and another one bent to the side (left or right). Then the model was loaded vertically on the top surface of the L5 vertebra. The results obtained were very similar to the ones of the phases 3 and 4.
Rotatory forces were not examined since there was a lack of data necessary for such loading.

6. Results.

The resulting stress and strain conditions from the application of the uniform load of 0.4Mpa at the upper surface of L5, is shown in Figures 7 and 8, while quantitative information for the strain size and statistics for the upper surface of L5 is given in Tables I, II, III and IV and Figures 5 and 6.

From Table 1 we find that the mean displacements along the axes x, y, z are –0.14mm, -0.161mm and –0.952mm, respectively, while the corresponding standard deviations are 0.010mm, 0.026mm and 0.035mm. The mean displacement of the nodes is 0.967mm and the standard deviation 0.038mm.

From Table II we find that the mean displacements along the axes x, y, z are –0.024mm, -0.166mm and -0.946mm, respectively, while the corresponding standard deviations are 0.031mm, 0.020mm and 0.037mm. The mean 3-D displacement of the nodes is 0.961mm and the standard deviation 0.040mm.

Figure 5. Strain of nodes along the three axes. The node numbers can be seen in Fig. 6. The displacement along the y-axis is half an order of magnitude larger than along the y-axis, while the displacement along the z-axis is the largest by far and as expected taking into consideration the direction of the applied load.

TABLE I. An example of 3-d displacements of node Position co-ordinates (mm)

NODE No	u_x	u_y	u_z	u	NODE No	u_x	u_y	u_z	u
1	-0.0357	-0.1320	-0.9682	0.9778	35	-0.0151	-0.1407	-0.9271	0.9378
2	-0.0291	-0.1288	-0.9507	0.9598	41	-0.0089	-0.1347	-0.9025	0.9125
3	-0.0085	-0.1835	-1.0028	1.0195	42	-0.0121	-0.1835	-0.9987	1.0154
4	-0.0207	-0.1728	-0.9752	0.9906	43	-0.0142	-0.1698	-0.9629	0.9779
5	-0.0217	-0.1565	-0.9550	0.9679	44	-0.0107	-0.1540	-0.9397	0.9523
6	-0.0261	-0.1392	-0.9444	0.9550	45	-0.0103	-0.1417	-0.9214	0.9323
7	0.0000	-0.2254	-1.0098	1.0346	51	-0.0033	-0.1379	-0.8935	0.9040
8	-0.0245	-0.1779	-0.9796	0.9959	52	-0.0119	-0.1848	-0.9990	1.0160
9	-0.0235	-0.1578	-0.9604	0.9735	53	-0.0097	-0.1745	-0.9604	0.9761
10	-0.0292	-0.1417	-0.9520	0.9630	54	-0.0079	-0.1531	-0.9373	0.9498
21	-0.0212	-0.1306	-0.9255	0.9349	55	-0.0048	-0.1438	-0.9184	0.9296
22	-0.0114	-0.1835	-1.0020	1.0187	61	0.0032	-0.1392	-0.8894	0.9003
23	-0.0143	-0.1727	-0.9696	0.9850	62	-0.0335	-0.2317	-1.0028	1.0297
24	-0.0192	-0.1530	-0.9482	0.9607	63	-0.0081	-0.1672	-0.9572	0.9717
25	-0.0208	-0.1393	-0.9348	0.9454	64	-0.0023	-0.1537	-0.9353	0.9478
31	-0.0146	-0.1328	-0.9118	0.9215	65	0.0008	-0.1452	-0.9158	0.9272
32	-0.0196	-0.2204	-1.0071	1.0311	71	0.0109	-0.1398	-0.8884	0.8994
33	-0.0148	-0.1690	-0.9649	0.9797	72	-0.0085	-0.1854	-0.9978	1.0149
34	-0.0144	-0.1522	-0.9435	0.9558					

TABLE II. Another example of 3-d displacements of node position co-ordinates (mm)

NODE No	u_x	u_y	u_z	u	NODE No	u_x	u_y	u_z	u
73	-0.0074	-0.1689	-0.9569	0.9717	111	0.0498	-0.1512	-0.8929	0.9069
74	0.0027	-0.1553	-0.9334	0.9462	112	-0.0016	-0.1881	-1.0063	1.0237
75	0.0076	-0.1449	-0.9137	0.9251	113	0.0148	-0.1714	-0.9552	0.9705
81	0.0199	-0.1402	-0.8885	0.8997	114	0.0350	-0.1536	-0.9383	0.9514
82	-0.0093	-0.1863	-1.0003	1.0175	115	0.0441	-0.1533	-0.9222	0.9358
83	-0.0015	-0.1739	-0.9546	0.9703	121	0.0611	-0.158	-0.9013	0.9170
84	0.0086	-0.1521	-0.9321	0.9444	122	-0.0546	-0.2212	-1.0169	1.0421
85	0.0160	-0.1459	-0.9122	0.9239	123	0.0339	-0.1619	-0.9549	0.9691
91	0.0311	-0.1423	-0.8890	0.9008	124	0.0436	-0.1593	-0.9452	0.9595
92	-0.0529	-0.2332	-1.0074	1.0353	125	0.0545	-0.1581	-0.9317	0.9465
93	0.0085	-0.1623	-0.9516	0.9653	131	0.0734	-0.1688	-0.9132	0.9315
94	0.0172	-0.1535	-0.9334	0.9460	132	0.0039	-0.1893	-1.0114	1.0289
95	0.0251	-0.1475	-0.9133	0.9254	133	0.0311	-0.1692	-0.9614	0.9766
101	0.0412	-0.1469	-0.8903	0.9032	134	0.0550	-0.1639	-0.9513	0.9668
102	-0.0038	-0.1877	-1.0022	1.0196	135	0.0668	-0.1627	-0.9424	0.9586
103	0.0078	-0.1660	-0.9545	0.9688	141	0.0903	-0.1770	-0.9321	0.9530
104	0.0257	-0.1554	-0.9346	0.9477	142	0.0050	-0.1912	-1.0168	1.0346
105	0.0346	-0.1487	-0.9165	0.9291	143	0.0398	-0.1771	-0.9633	0.9802

From Fig. 5 we conclude that the displacements along the axes x and y are small with the displacement along the y-axis being systematically larger. Also, that the vertical displacement is by almost one of order of magnitude larger. The maximum displacement along the three axes are, respectively, 0,09mm -0,23mm, and 1,04mm. Figure 8 gives the vertical displacement of the nodes of the upper L5 surface using as insert a colour key.

The mean normal stresses along the axes x, y and z at the positions of the listed nodes are –0.024, 0.258 and –0.369, respectively, and the corresponding standard deviations are 0,136, 0,331 and 0,195. Also, the mean normal stresses along the axes x, y and z are 0.017, -0.027 and 0.022, respectively and the corresponding standard deviations are 0.119, 0.076 and 0.046. Figure presents the equivalent von Mises stress at the upper surface of L5 using as insert a colour key.

TABLE III. An example of normal and shear stress components along axes and planes at node positions (in mpa units)

Node No	S_x	S_y	S_z	S_{xy}	S_{yx}	S_{xz}
1	-0.0127	0.0593	-0.4975	-0.0194	-0.1504	0.0562
1	-0.0127	0.0593	-0.4975	-0.0194	-0.1504	0.0562
1	-0.0127	0.0593	-0.4975	-0.0194	-0.1504	0.0562
2	-0.0109	0.0477	-0.5737	-0.0235	-0.1035	0.0510
2	-0.0109	0.0477	-0.5737	-0.0235	-0.1035	0.0510
3	-0.3690	-0.0968	-0.6059	0.1158	0.0410	0.0477
3	-0.3690	-0.0968	-0.6059	0.1158	0.0410	0.0477
4	0.0871	0.1365	-0.4253	-0.0099	-0.0085	--
5	-0.0074	0.2176	-0.4294	0.0016	-0.0225	--
6	0.0179	0.1536	-0.4186	-0.0261	-0.0474	--
7	-0.0538	0.8968	-0.2082	-0.1144	0.1649	0.1410
7	-0.1752	0.954	-0.1965	0.2932	-0.1251	0.0977
7	-0.2408	0.5263	-0.2581	-0.2246	0.0317	0.1364
7	-0.049	0.1790	-0.0466	0.2635	0.1858	--
8	0.1665	0.6367	-0.2863	0.0261	-0.0278	-0.0118
8	0.1665	0.6367	-0.2863	0.0261	-0.0278	-0.0118
9	0.0007	0.2720	-0.3651	0.0043	-0.0237	-0.0025
9	0.0007	0.2720	-0.3651	0.0043	-0.0237	-0.0025
10	0.0084	0.1632	-0.3428	-0.0268	-0.0671	-0.0046
10	0.0084	0.1632	-0.3428	-0.0268	-0.0671	-0.0046
11	0.0228	0.0583	-0.4382	-0.0208	-0.0441	0.0419
11	0.0228	0.0583	-0.4382	-0.0208	-0.0441	0.0419
12	-0.2801	0.0701	-0.5884	-0.1923	0.0641	-0.0400
12	-0.2801	0.0701	-0.5884	-0.1923	0.0641	-0.0400
13	-0.0025	0.1653	-0.4307	-0.0251	-0.0241	0.0161
24	0.0223	0.2012	-0.4060	-0.0016	-0.0203	-0.0191
25	0.0218	0.1005	-0.4182	-0.0192	-0.0275	-0.0215
31	0.0170	0.0437	-0.3885	-0.0123	-0.0331	0.0111
31	0.0170	0.0437	-0.3885	-0.0123	-0.0331	0.0111
32	0.1623	0.9556	-0.1959	0.1715	-0.1324	-0.0118
32	0.0991	1.2563	-0.0984	0.2349	0.0293	-0.0041
32	0.1170	-0.0449	0.4236	0.2635	-0.0478	--
33	0.0497	0.5336	-0.3342	0.0962	-0.0058	-0.0004
34	0.0373	0.1593	-0.3882	0.0013	-0.0248	-0.0137
35	0.0149	0.0780	-0.4020	-0.0114	-0.0293	-0.0136

In table IV you see an example of pressure loadings for different angles that were used during the experiment. Each test resulted in a database of node displacements that depicted the model's final condition.

TABLE IV

LOADING \ ANGLE	ONLY ONCE	REPETITIVE, AFTER RETURNING TO INITIAL POSITION	REPETITIVE, BEFORE RETURNING TO INITIAL POSITION
0^0			
10^0			
20^0			
30^0			
45^0			

7. Conclusions.

The FE model of the critical lumbar group of the L5, S1 and the in-between disk, presented in this paper that consists of 15000 elements and 27000 nodes and can be loaded by multidirectional and time-dependent external force, after a limited number of applications appears to represent reality of the structure and processes and deserves further experimentation and comparative evaluation of results.

The application of a vertical compression load upon the upper surface of L5 using this model discloses development of normal and shear stresses at the nodes of magnitude one order, or even higher, than that of the external load. Impressive is the magnitude of the normal stresses along the y-axis, which is systematically larger than those along the x-axis. The node displacements follow the same pattern, namely, considerable (almost one order of magnitude larger than the rest) is the displacement along the z-axis, while the displacement along the y-axis is systematically larger than the ones along the x-axis. The higher the initial load, the greater was the deformation of the disk. However, when the load became extremely high, the cancellus first and the cortical later, bone was deformed, showing macroscopically a condition similar to fracture of the L5 vertebra.

FE analysis for time-dependent loading requires discretization of the time parameter, using fixed or variable time-step h, and repetitive runs of the programme. The need to define the state of the FE model as strained by the loading of the previous run plays important role. The loading model developed in this paper, simulates multidirectional and time-dependent compression **P,** including quasi-periodic vibration cases, as well as cases of shock loading. Indeed, loading and analysing at discrete instant t_n the FE model, the latter under state of deformation, full or partial, caused by the loading at the instant $t_n – h$, a realistic simulation of resonant as well as non-resonant external loading and impacts is secured.

The application of non-vertical compression loads upon the upper surface of L5 using this model discloses development of smaller normal and greater shearing stresses at the nodes, of magnitude many orders than that of the external load. With this form of loading, greater angles resulted to greater deformation of the disk, given the same pressure loading. Also, when the initial loads were comparatively high, a deformation of the geometry of the entire system was noticed, showing a macroscopic similarity with true spondylolisthisis. This result was limited when the parameters refering to the damping and boundary conditions of the surrounding tissues were increased, highlighting the importance of these tissues for the proper operation of the disk-vertebra system, in the model and most probably in the human spine as well.

The application of vertical compression loads but on an already deformed disk, simulating different stances, showed similar results with the application of non-vertical loads. With this form of loading the model showed that, given the same loading pressure, the disk was deformed proportionaly to the angle of initial deformation. Plastic deformation of the disk was rather easily achieved with comparatively low loads the “bending” of the model reached its anatomical maximum. This form of loading needs further investigation.

At this point there are only few results that can be safely stated:

- The intervertebral disk can tolerate extreme loads on the vertical (z) axis, as long as the posture of the model is appropriate. The vertebrae rather than the disk will suffer damage with such loadings.
- The posture of the model seems the most important factor affecting the resulting deformations for the same load.
- Non-vertical loads deform the morphology of the entire model (lumbar spine) showing the importance of the surrounding tissues, as dumping and protective factors.

8. References.

Goudas P, Pope M, Labeas G, Macropoulos V, Goudas, CL. Development and Analysis of a FE Model for the F5/S1 Disk , Using a Loading Model Simulating WBV. (Submitted also to Vibration Injury Network as a final report)

Seidel H, Blüthner R, Hinz B, Schust M. Stresses in the lumbar spine due to whole-body vibration containing shocks, Publisher: Bundesanstalt für Arbeitsschutz und Arbeitsmedizin Fachbereich Arbeitsmedizin, Sitz Berlin Nöldnerstraße 40-42, 10317 Berlin Postfach 5, 10266 Berlin 1998.

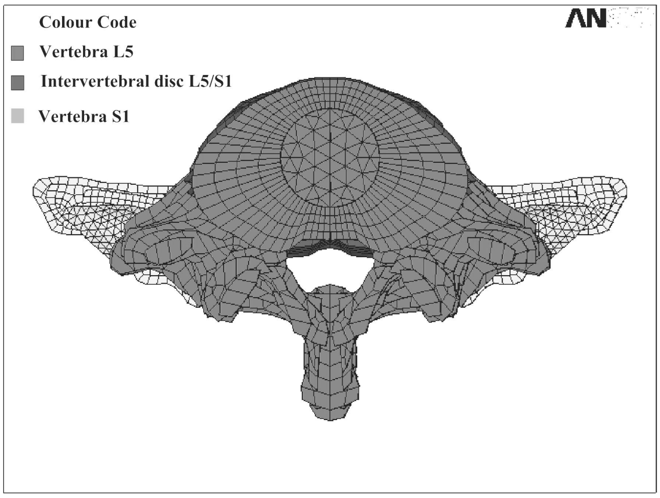

Figure 1. Perspective view from top-front of the spine group L5, L5/S1 disc and S1, in the form of FE model. The group is partitioned into a total of 14906 elements.

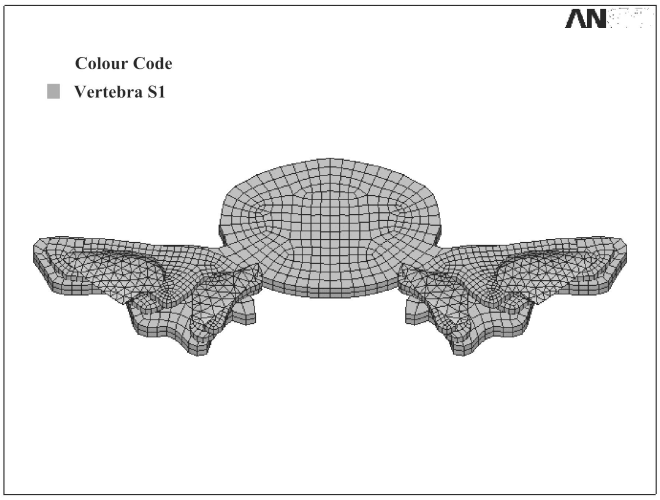

Figure 2. Perspective view from top-front of the upper segment of the vertebra S1. This vertebra is partitioned into 3722 elements.

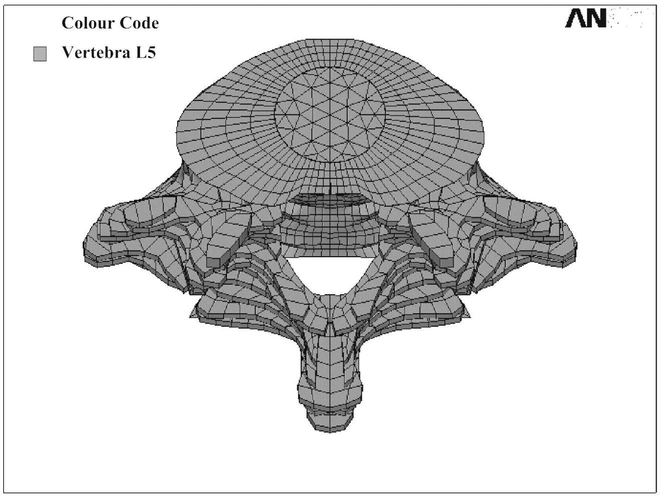

Figure 3. Perspective view from top-front of the vertebra L5 as it is included in the FE model appearing in Figure 1. This vertebra is partitioned into 9432 elements.

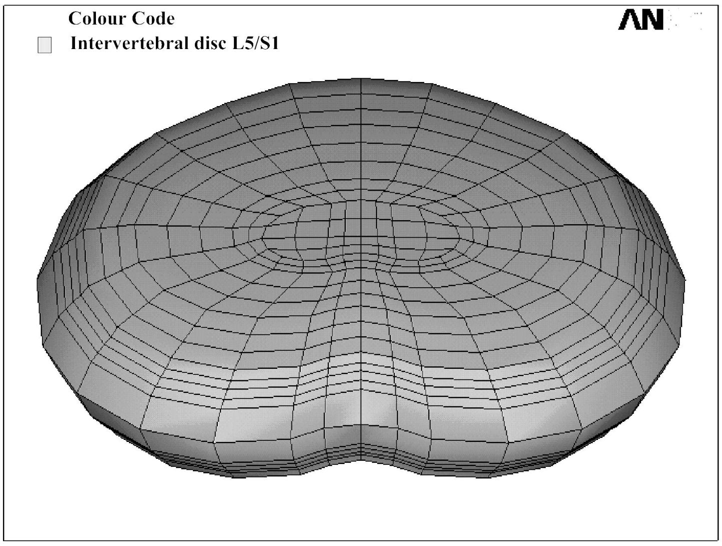

Figure 4. Perspective view from top-front of the L5/S1 intervertebral disk which is partitioned into 1752 elements.

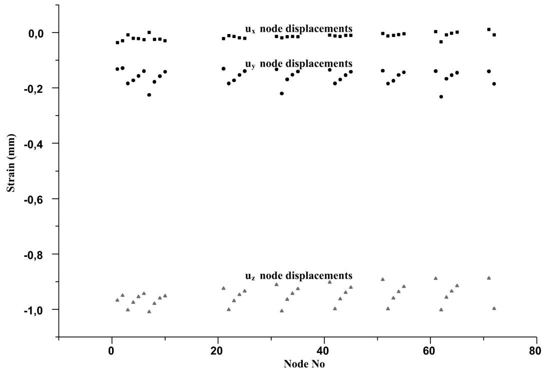

Figure 5. Strain of nodes along the three axes. The node numbers can be seen in Fig. 6. The displacement along the y-axis is half an order of magnitude larger than along the y-axis, while the displacement along the z-axis is the largest by far and as expected taking into consideration the direction of the applied load.

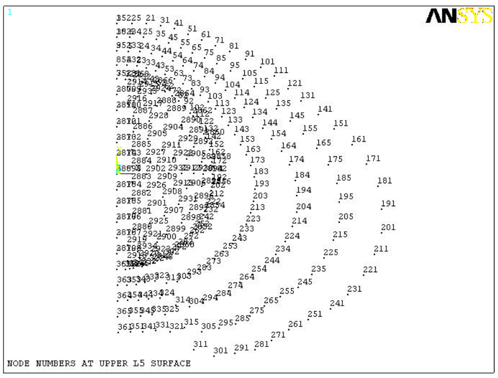

Figure 6. Node No's at upper L5 surface related to the strain results listed in Table I.

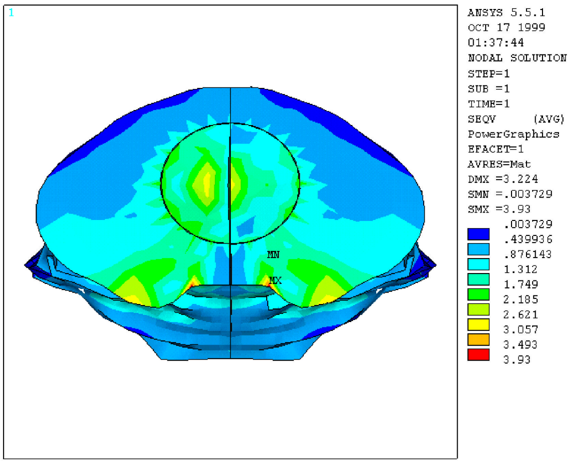

Figure 7. The equivalent von Mises stress at the upper surface of L5.

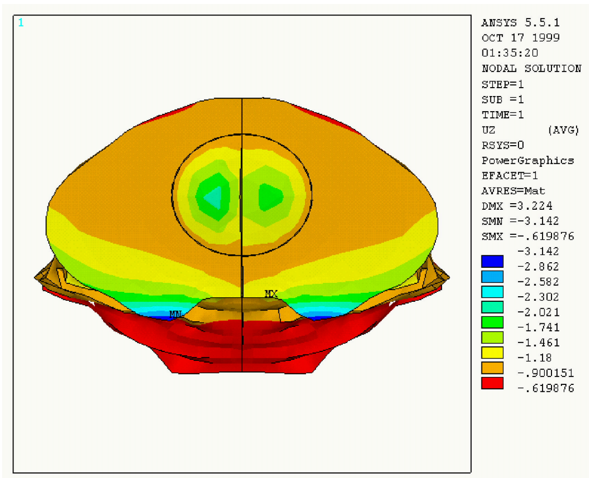

Figure 8. Displacement u_z (vertical axis) of the disk (in mm).